

VLBA discovery of a resolved source in the candidate black hole X-ray binary AT2019wey

NITIKA YADLAPALLI,¹ VIKRAM RAVI,¹ YUHAN YAO,¹ S. R. KULKARNI,¹ AND WALTER BRISKEN²

¹ *Cahill Center for Astronomy and Astrophysics, California Institute of Technology, Pasadena, CA 91125, USA*

² *National Radio Astronomy Observatory, Socorro, NM 87801, USA*

ABSTRACT

AT2019wey is a Galactic low mass X-ray binary with a candidate black hole accretor first discovered as an optical transient by ATLAS in December 2019. It was then associated with an X-ray source discovered by SRG in March 2020. After observing a brightening in X-rays in August 2020, VLA observations of the source revealed an optically thin spectrum that subsequently shifted to optically thick, as the source continued to brighten in radio. This motivated observations of the source with the VLBA. We found a resolved source that we interpret to be a steady compact jet, a feature associated with black hole X-ray binary systems in the hard X-ray spectral state. The jet power is comparable to the accretion-disk X-ray luminosity. Here, we summarize the results from these observations.

Keywords: Low-mass x-ray binary stars, Black holes, Very long baseline interferometry

1. INTRODUCTION

Black hole X-ray binaries are comprised of stellar mass black holes accreting from companion stars. Radio observations of these systems are crucial to identifying the presence of relativistic jets and studying disk/jet coupling. Disk/jet coupling is the idea that a conservation of mass and energy analysis can place constraints on the physical properties of a radio jet given knowledge of the accretion rate in the disk. The presence of a jet is dependent on which X-ray spectral state the black hole binary is observed to be in (Fender 2001). The two main states of interest are the thermal state (formerly known as the high/soft state) and the hard state (formerly known as the low/hard state). The thermal state is dominated by a thermal spectrum, with greater than 75% of the observed flux being contributed by the accretion disk. The thermal spectrum is accompanied by a steep power law extending to energies higher than ~ 10 keV. In the hard state, which is associated with the presence of compact jets, the disk contributes very weakly and greater than 80% of the flux is contributed by a nonthermal power law spectrum. The spectrum is characterized by a photon index of $1.4 < \Gamma < 2.1$. In this state the accretion disk appears cooler and correlations between radio and X-ray fluxes are observed. For a more detailed explana-

tion, see Fender (2003), McClintock & Remillard (2009), and Remillard & McClintock (2006).

The first observation of a resolved steady jet in an X-ray binary was conducted with the Very Large Array (VLA) on SS 433 (Hjellming & Johnston 1981). SS 433 was the first discovery of a microquasar, a radio-luminous X-ray binary that is the low-mass analog to a quasar. Subsequent observations of microquasars GRS 1915+105 (Mirabel & Rodríguez 1994) and GRO 1655 – 40 (Tingay et al. 1995), with the VLA and the Southern Hemisphere VLBI Experiment (SHEVE) respectively, following radio and X-ray outbursts revealed the first examples of superluminal motion in our galaxy and provided more insight into the notion of disk/jet coupling. These discoveries along with consistent monitoring of such systems helped construct a unified model of radio jets in black hole binaries (Fender et al. 2004). Systems observed in the thermal state have been seen to have detached, highly relativistic ejecta as in the previously mentioned sources. As these systems are observed to evolve along a track from a high to low hardness, it is thought that systems in the hard state are associated with compact jets and only mildly relativistic bulk motion.

To date, however, compact steady jets have only been spatially resolved in the hard states for two high-mass X-ray binaries, GRS 1915+105 (Dhawan et al. 2000) and Cyg X-1 (Stirling et al. 2001), and one low-mass X-ray binary, MAXI J1836–194 (Russell et al. 2015). In the case of the high-mass X-ray binary systems, where the

flux density of the radio sources is high and the resolved jet is many times larger than the synthesized beam of the observation, quantities such as distance to the system, jet power, and jet speed can be derived. Such observations are consistent with the model of conical synchrotron jets to describe radio emission from black hole candidate systems (Hjellming & Johnston 1988) and supported the derivation of scaling relations between jet power and accretion disk luminosity (Falcke & Biermann 1995; Falcke & Biermann 1999). Adding to the handful of spatially resolved black hole X-ray binary jets in the low/hard state is critical towards refining physical models for disk/jet coupling.

AT2019wey was first discovered as an optical transient by the Asteroid Terrestrial-impact Last Alert System (ATLAS) on December 7, 2019 (Tonry et al. 2019). A few months later on March 18, 2020, Spektrum-Roentgen-Gamma (SRG) discovered an X-ray source coincident with the position of the ATLAS detection (Mereminskiy et al. 2020). The discovery of hydrogen absorption lines with a redshift $z = 0$ favored a Galactic origin for the source and led Yao et al. (2020b) to posit a Galactic accreting binary origin. Detailed analysis of the X-ray spectra and light curves as well as a multiwavelength follow-up campaign of the source is described in Yao et al. (2020c) and Yao et al. (2020d). High optical luminosity as well as the ratio of the optical and X-ray luminosities, which was well above that expected for a neutron star companion, supported a black hole accreting object. An analysis of historical optical magnitudes suggests an upper limit of $0.8M_{\odot}$ for the companion mass. The system is expected to have a low inclination angle of $i \lesssim 30^{\circ}$ and a distance of between 1–10 kpc. On August 2, 2020, VLA observations of AT2019wey revealed an optically thin spectrum from 1–12 GHz, which stood in contrast with the previous measurements of an optically thick spectrum on May 27, 2020 (Yao et al. (2020a) and Cao et al. (2020)). The optically thin spectrum coupled with a recent X-ray flare suggested a transition to a higher bulk Lorentz factor in the jet and the possibility of ejected components. Subsequent radio spectra taken on August 14, 21, and 28 showed a return to an optically thick spectrum and a flux density that continued to increase. This motivated us to pursue observations of AT2019wey with the Very Long Baseline Array (VLBA) to resolve this rapidly evolving radio source.

The rest of the paper is organized as follows. Section 2 provides details on our VLBA observation as well as our data analysis procedure and Section 3 summarizes the observed properties of AT2019wey. Section 4 discusses parallels between AT2019wey and MAXI J1836–194

and provides an analysis of the minimum energy and power of the system.

2. OBSERVATION AND ANALYSIS PROCEDURES

Two epochs of 6 cm observations of AT2019wey were obtained with the Very Long Baseline Array (VLBA) on September 6, 2020 and September 12, 2020 and processed with the DiFX correlator (Deller et al. 2011). Our observations (marked by red stars), are shown alongside radio and X-ray light curves of AT2019wey in Fig 1. The radio observations were taken with the VLA, except for the last measurement which was conducted with the European VLBI Network (EVN) by Giroletti et al. (2020). All measurements were scaled to 4.8 GHz using the spectral indices published by Yao et al. (2020d). The X-ray count rates show measurements taken by the Monitor of All-sky X-ray Image (MAXI) telescope in the 2–10 keV band (Matsuoka et al. 2009). Both three hour epochs were phase referenced, with alternating scans of 3.5 minutes on AT2019wey and 40 seconds on the phase reference (J0418+5457). The phase reference is at an assumed location of RA = $04^{\text{h}}18^{\text{m}}19.3401920^{\text{s}}$ and Dec = $54^{\circ}57'15.334490''$, an angular separation of 2.47° from the target, and was chosen because of its inclusion in the third realization of the International Celestial Reference Frame (ICRF3) (Charlot et al. 2020). Each epoch also contained about 4 minutes of time on a check source (J0427+5618) and 6 minutes of time on a bandpass calibrator (J0555+3948). During this time, data was only recorded in two of the four spectral windows at the Pie Town antenna; this station was flagged for the analysis presented in this paper. Calibration and imaging for the observations was carried out in AIPS (Greisen 2003). Phase solutions were derived for both the check source and AT2019wey by first performing global fringe fitting on the phase calibrator. Then we performed two rounds of phase-only self-calibration and one round of amplitude+phase self-calibration with two minute solution intervals, assuming a point source model with the published flux density for the source. Once relatively flat phase solutions were reached, with variations less than $\pm 5^{\circ}$ for all stations, these phase solutions were applied and no further self-calibration was performed on either the check source or AT2019wey. All images were created with natural weighting to maximize sensitivity. Images of the phase calibrator and check source are shown in Fig 2 and images of AT2019wey are shown in Fig 3. The full-width half maximum of the Gaussian model used to approximate the synthesized beam (shown in corners of the images), and was convolved with the CLEAN components in the images, is approximately a $4 \text{ mas} \times 1.5 \text{ mas}$ ellipse in both epochs. The

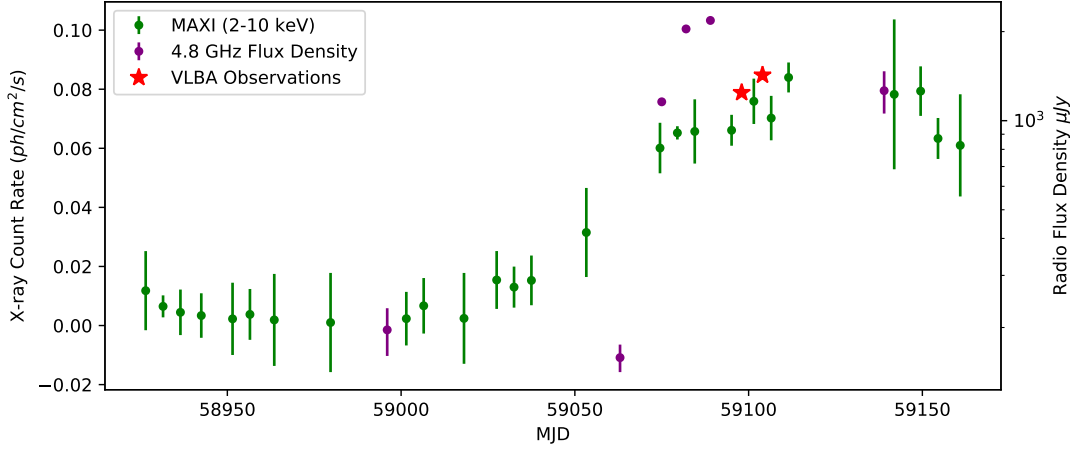


Figure 1. Lightcurves showing radio observations (scaled to 4.8 GHz) and X-ray observations from MAXI (2-10 keV). The red stars on the plot show the observations discussed in this work.

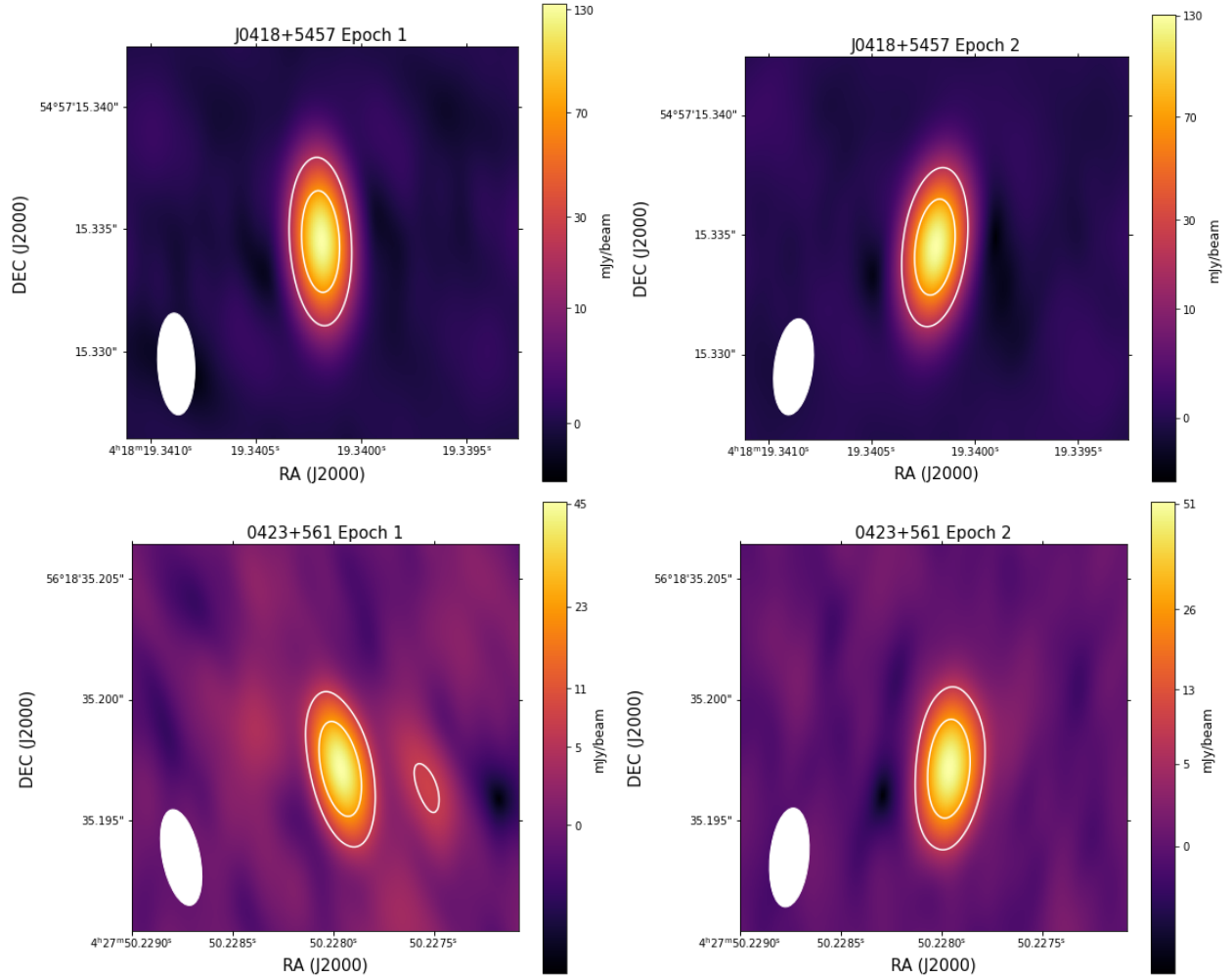


Figure 2. CLEAN images of the phase reference (top row), J0418+5457, and the check source (bottom row), 0423+561, for both epochs. The images are consistent with point sources. Also depicted on the images are 15% and 50% flux density contours.

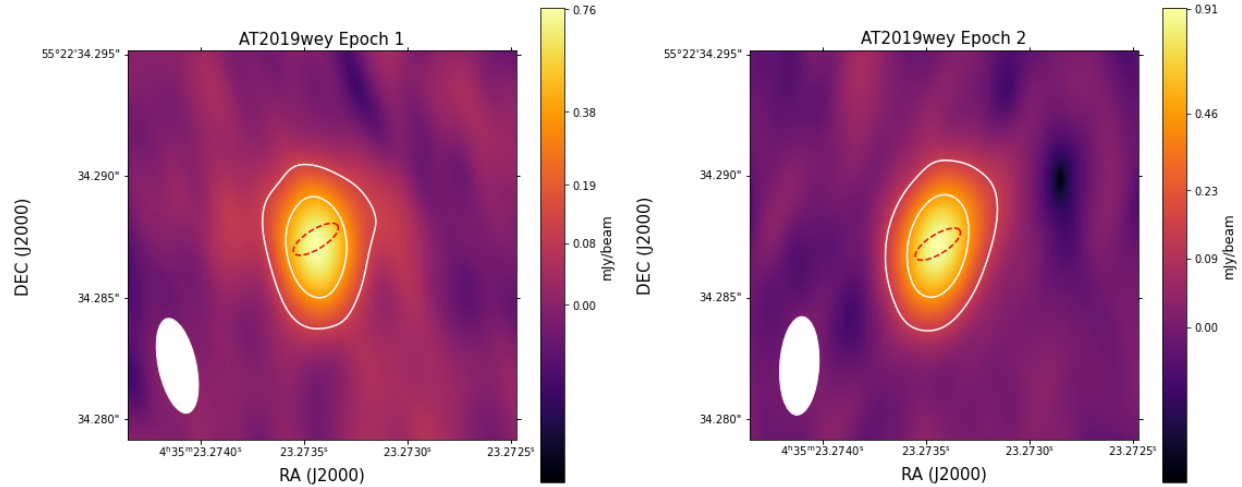


Figure 3. CLEAN images of AT2019wey for both epochs with 15% and 50% flux density contours. The red dotted line represents the single best fit deconvolved ellipse across both epochs for the source.

estimated deconvolved component (averaged across both epochs) is also represented by the red dotted ellipse in Fig 3.

3. RESULTS

Both the images and uv-amplitudes of AT2019wey show that the source is resolved. An initial inspection of the images (Fig 3) shows a source that is clearly wider and oriented at a different position angle than the elliptical model of the synthesized beam. Additionally, plots of the uv-amplitudes, coherently averaged for 20 minute intervals and shown in Fig 4 along with uncertainties, do not show a flat amplitude distribution as would be expected from a point source. Thus, we attempted to fit a Gaussian component to the visibilities using the `uvfit` task in AIPS; however, low signal to noise in individual visibility measurements yielded unreliable results for a Gaussian model fit to the uv-plane.

Instead of fitting to the uv-amplitudes, we performed an image plane fit using `jmfit` in AIPS. To start, we split each epoch into hour long blocks to investigate any time variability in the source. For each block, we use `jmfit`, which uses a least squares approach to fit a single Gaussian component to the image and then deconvolves the CLEAN beam from the fitted component to estimate a Gaussian model for the true source geometry. For each source, we fixed the position of the source to the phase center. The `jmfit` task also provides uncertainties for all of these parameters; however, the task will report the lower limits of the deconvolved major and minor axis as 0 mas if a reliable uncertainty cannot be derived. In this case, we use the upper limit error when calculating a single best fit value for the major and minor axis sizes. Additionally, the best fit parameters are anomalous for the first hour of the first epoch, so these are omitted

in the calculation of the single best fit value for each parameter. Inspection of the phase calibrator shows no significant phase or gain fluctuations during this time, indicating that the anomalous measurement is likely not caused by calibration error. As a light-crossing time of one hour is equivalent to a distance of several AU, it cannot be ruled out that this measurement is due to true variability in the X-ray binary. The use of dynamical imaging, left to a later work, would provide a way to verify such short timescale evolution. The fitted flux density, position angle reported east of north, the major axis, and the minor axis for each hour of both epoch is shown along with uncertainties in Fig 5. The single best fit values are summarized in Table 1.

Aside from the first hour of epoch 1, the source geometries of AT2019wey remain consistent within the uncertainties across both epochs. The fitted flux density of AT2019wey, however, is around 15% higher in the second epoch than the first. As the source is seen to be fading in the radio lightcurve presented in Yao et al. (2020d), we do not expect the second epoch to show significant increase in brightness. A similar level of variation is seen in the flux density of the check source, which was fitted to 45.6 mJy in epoch 1 compared to 54.9 mJy in epoch 2. This may indicate residual phase error in the first epoch 1 leading to a lower flux density measurement, but intrinsic source variability on these small angular scales cannot be ruled out.

4. DISCUSSION

Prior to these observations of AT2019wey, a resolved compact jet in a black hole low-mass X-ray binary was only observed in one other source, MAXI J1836–194. Drawing upon the analysis conducted in Russell et al. (2015), we find many useful parallels between the two

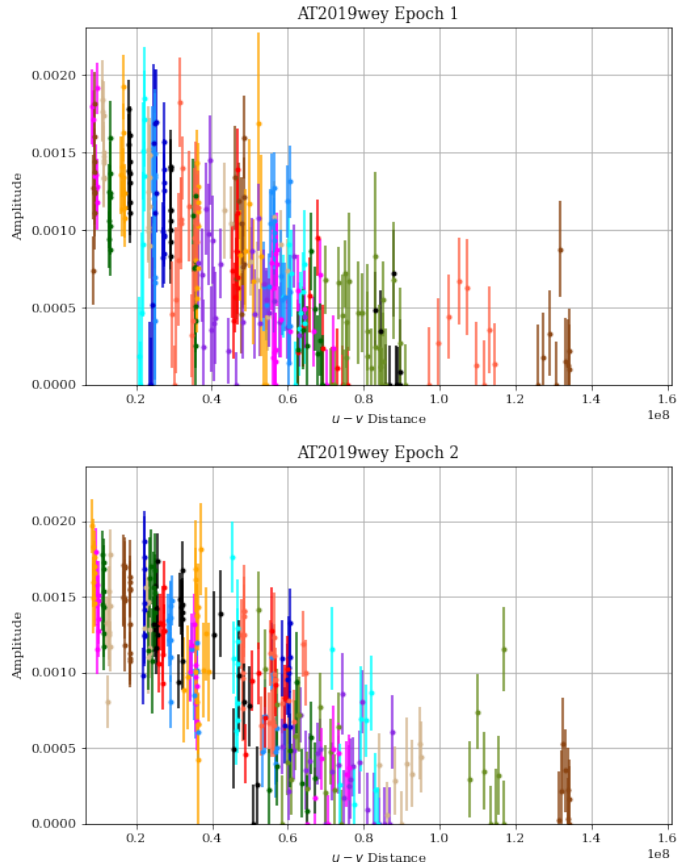


Figure 4. UV-amplitudes of AT2019wey for both epochs, with colorized points representing different baseline pairs.

Table 1. Source Properties for AT2019wey

RA (J2000)	Dec (J2000)	Flux Density	Major Axis	Minor Axis	Position Angle
04 ^h 35 ^m 23.2734 ^s	55°22′34.287″	1.35 ± 0.02 mJy	2.13 ± 0.10 mas	0.80 ± 0.18 mas	122° ± 4°

sources, both of which are low inclination systems with poor distance constraints. VLBA observations were obtained of both sources around periods of brightening in X-ray and radio fluxes when the systems were thought to be in the hard state. Both of these observations show marginally resolved extended structure. In the five epochs of observations, the angular scale of the MAXI J1836–194 jet was seen to evolve as the radio flux density rose and faded. At 8.42 GHz, a maximum major axis of 0.699 mas was measured at a peak flux density of 38.5 mJy. It is interesting to note that MAXI J1836–194 showed a steeply rising radio spectral index of $\alpha \sim 0.6 - 0.8$ ¹, compared to AT2019wey which showed $\alpha \sim 0.2$ in the week prior to our observa-

tions. Detached ejecta were not observed in either system as well. In our case, VLBA observations were taken a month after the initial observation of an optically thin spectrum with the VLA. Thus, any relativistically moving ejecta would have already been well outside of our field of view. Observations closer to the proximity of the flare event may have revealed such ejecta. In the case of MAXI J1836–194, however, though the radio spectral index became shallower as the source transitioned from the hard state to the hard intermediate state, the spectrum never became optically thin, leading Russell et al. (2015) to suggest that the increase in flux was due to a failed outburst event.

It is likely that the radio emission we observe is dominated by the synchrotron mechanism. The consistency between the VLBA and roughly coeval VLA (Yao et al.

¹ $f_\nu \propto \nu^\alpha$

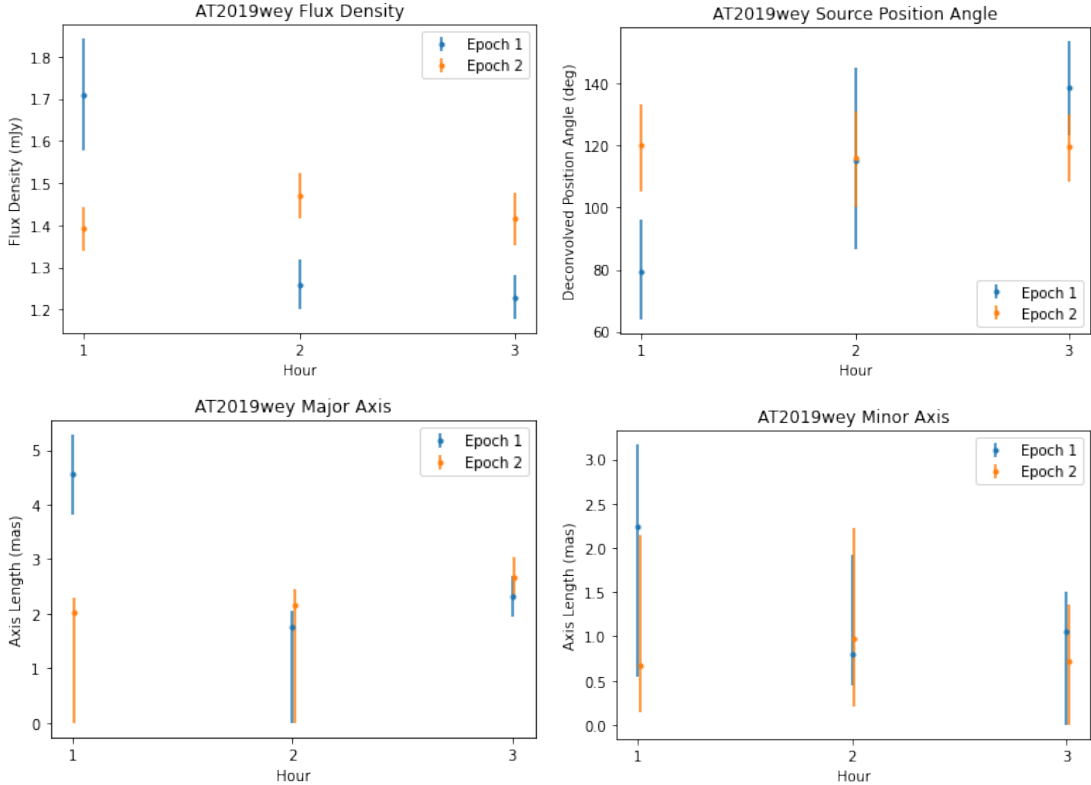


Figure 5. Model parameters derived for a Gaussian image plane fit to hour long observation blocks of AT2019wey. All of the geometric parameters are estimations of a deconvolved component. Top left: flux density, top right: position angle measured east of north, bottom left: major axis, bottom right: minor axis

2020d) flux densities implies that the VLA spectral measurements can be applied to the VLBA source. The variability of the radio spectral shape, and in particular the observation of a steeply negative spectrum with index $\alpha = -0.8 \pm 0.2$, argues against a bremsstrahlung origin for the radio emission. This is consistent with previous observations of hard-state black hole X-ray binaries (Dhawan et al. 2000; Russell et al. 2015). We defer a full-polarization analysis of our VLBA data to a future work.

The measurement of an angular size enables us to estimate the total energy in the source following standard synchrotron theory (e.g., Pacholczyk 1970). Assuming flat-spectrum between 1–12 GHz only (spanning the VLA observations of AT2019wey) with a flux density of 1.35 mJy, a fiducial distance of $D = 3$ kpc, a corresponding source volume of 10^{42} cm^{-3} (based on the measured angular size), the minimum energy required to power the synchrotron source (relativistic particles and magnetic fields) is

$$E_{\min} \approx 5 \times 10^{38} \left(\frac{D}{3 \text{ kpc}} \right)^{\frac{17}{7}} \text{ erg.} \quad (1)$$

The corresponding mean magnetic field strength is ~ 0.07 G, implying a relativistic-lepton Lorentz factor of

$\gamma \approx 250$ for 12 GHz emission. Assuming a characteristic particle acceleration timescale corresponding to the light crossing time of the source of $\sim 3 \times 10^3$ s at 3 kpc, the power dissipation in the source is approximately

$$P \gtrsim 2 \times 10^{35} \left(\frac{D}{3 \text{ kpc}} \right)^{\frac{10}{7}} \text{ erg s}^{-1}. \quad (2)$$

We emphasize that this is a lower limit given the limited band used to calculate the total radio luminosity, and the minimum-energy assumption.

The inferred power is remarkably close to the $\sim 10^{36} \text{ erg s}^{-1}$ X-ray luminosity of AT2019wey inferred by Yao et al. (2020c) for a 3 kpc distance. The luminosity of the thermal emission from the disk is likely a few tens of percent of this total. This correspondance has been observed previously in the hard and plateau states of the high-mass X-ray binary GRS 1915+105 (e.g., Dhawan et al. 2000), and is a critical assumption of models for symbiotic disk-jet systems (Falcke & Biermann 1999). Although we resolve the radio source in AT2019wey, we have no compelling morphological evidence for a jet. Nonetheless, the panchromatic properties of AT2019wey are closely similar to low-mass black hole X-ray binaries in which relativistic jets have been observed (Yao et al. 2020d). We therefore interpret the resolved source as a

compact steady jet, with a power that is comparable to the accretion-disk X-ray luminosity.

5. CONCLUSION

We present here two epochs of 6 cm VLBA observations of candidate black hole low-mass X-ray binary system AT2019wey following a period of X-ray and radio brightening. The observations revealed a marginally resolved source with deconvolved source geometries that are relatively constant across both epochs. Together with the observed X-ray spectrum, we interpret these results to indicate the presence of a compact, steady jet. Using the angular scale derived from image plane fits of

a Gaussian component to the source, we show that the power dissipation from the jet is comparable to the X-ray luminosity, consistent with a standard assumption of models for disk/jet coupling.

6. ACKNOWLEDGEMENTS

We thank Tim Pearson, Gregg Hallinan, and Katie Bouman for useful discussions on interpreting these results. These observations were conducted with the Very Long Baseline Array. The National Radio Astronomy Observatory is a facility of the National Science Foundation operated under cooperative agreement by Associated Universities, Inc. This research has made use of NASA's Astrophysics Data System.

REFERENCES

- Cao, H., Frey, S., Gabanyi, K., et al. 2020, *The Astronomer's Telegram*, 13984, 1
- Charlot, P., Jacobs, C. S., Gordon, D., et al. 2020, arXiv e-prints, arXiv:2010.13625.
<https://arxiv.org/abs/2010.13625>
- Deller, A. T., Brisken, W. F., Phillips, C. J., et al. 2011, *PASP*, 123, 275, doi: [10.1086/658907](https://doi.org/10.1086/658907)
- Dhawan, V., Mirabel, I. F., & Rodriguez, L. F. 2000, *The Astrophysical Journal*, 543, 373, doi: [10.1086/317088](https://doi.org/10.1086/317088)
- Falcke, H., & Biermann, P. L. 1995, *A&A*, 293, 665.
<https://arxiv.org/abs/astro-ph/9411096>
- Falcke, H., & Biermann, P. L. 1999, *Astronomy and Astrophysics*, 342, 49. <https://arxiv.org/abs/9810226>
- Fender, R. 2003, in *Compact Stellar X-ray Sources* (Cambridge University Press), 381–420, doi: [10.1017/cbo9780511536281.010](https://doi.org/10.1017/cbo9780511536281.010)
- Fender, R. P. 2001, *MNRAS*, 322, 31, doi: [10.1046/j.1365-8711.2001.04080.x](https://doi.org/10.1046/j.1365-8711.2001.04080.x)
- Fender, R. P., Belloni, T. M., & Gallo, E. 2004, *MNRAS*, 355, 1105, doi: [10.1111/j.1365-2966.2004.08384.x](https://doi.org/10.1111/j.1365-2966.2004.08384.x)
- Giroletti, M., Cao, H., An, T., et al. 2020, *The Astronomer's Telegram*, 14168, 1
- Greisen, E. W. 2003, *AIPS, the VLA, and the VLBA*, ed. A. Heck, Vol. 285, 109, doi: [10.1007/0-306-48080-8_7](https://doi.org/10.1007/0-306-48080-8_7)
- Hjellming, R. M., & Johnston, K. J. 1981, *The Astrophysical Journal*, 246, L141, doi: [10.1086/183571](https://doi.org/10.1086/183571)
- . 1988, *The Astrophysical Journal*, 328, 600, doi: [10.1086/166318](https://doi.org/10.1086/166318)
- Matsuoka, M., Kawasaki, K., Ueno, S., et al. 2009, *PASJ*, 61, 999, doi: [10.1093/pasj/61.5.999](https://doi.org/10.1093/pasj/61.5.999)
- McClintock, J. E., & Remillard, R. A. 2009, in *Compact Stellar X-ray Sources*, 157–214, doi: [10.1017/cbo9780511536281.005](https://doi.org/10.1017/cbo9780511536281.005)
- Mereminskiy, I., Medvedev, P., Semena, A., et al. 2020, *The Astronomer's Telegram*, 13571, 1
- Mirabel, I. F., & Rodríguez, L. F. 1994, *Nature*, 371, 46, doi: [10.1038/371046a0](https://doi.org/10.1038/371046a0)
- Pacholczyk, A. G. 1970, *Radio astrophysics. Nonthermal processes in galactic and extragalactic sources*
- Remillard, R. A., & McClintock, J. E. 2006, *X-ray Properties of Black-Hole Binaries*, Tech. rep.
- Russell, T. D., Miller-Jones, J. C., Curran, P. A., et al. 2015, *Monthly Notices of the Royal Astronomical Society*, 450, 1745, doi: [10.1093/mnras/stv723](https://doi.org/10.1093/mnras/stv723)
- Stirling, A. M., Spencer, R. E., De La Force, C. J., et al. 2001, *Monthly Notices of the Royal Astronomical Society*, 327, 1273, doi: [10.1046/j.1365-8711.2001.04821.x](https://doi.org/10.1046/j.1365-8711.2001.04821.x)
- Tingay, S. J., Jauncey, D. L., Preston, R. A., et al. 1995, *Nature*, 374, 141, doi: [10.1038/374141a0](https://doi.org/10.1038/374141a0)
- Tonry, J., Denneau, L., Heinze, A., et al. 2019, *Transient Name Server Discovery Report*, 2019-2553, 1
- Yao, Y., Dong, D., & Kulkarni, S. R. 2020a, *The Astronomer's Telegram*, 13921, 1
- Yao, Y., Enoto, T., Altamirano, D., et al. 2020b, *The Astronomer's Telegram*, 13932, 1
- Yao, Y., Kulkarni, S. R., Gendreau, K. C., et al. 2020c, arXiv e-prints, arXiv:2012.00160.
<https://arxiv.org/abs/2012.00160>
- Yao, Y., Kulkarni, S. R., Burdge, K. B., et al. 2020d, arXiv e-prints, arXiv:2012.00169.
<https://arxiv.org/abs/2012.00169>